International Journal of Rock Mechanics & Mining Sciences 49 (2012) 59–67

Contents lists available at SciVerse ScienceDirect

International Journal of Rock Mechanics & Mining Sciences

journal homepage: www.elsevier.com/locate/ijrmms

Initiation pressure, location and orientation of hydraulic fracture

Jinsong Huang [a,*], D.V. Griffiths [b], Sau-Wai Wong [c]

[a] Centre for Geotechnical and Materials Modelling, University of Newcastle, Callaghan, NSW 2308, Australia
[b] Division of Engineering, Colorado School of Mines, Golden, CO 80401, USA
[c] Shell International Exploration and Production, USA

ARTICLE INFO

Article history:
Received 7 December 2010
Received in revised form
12 October 2011
Accepted 20 November 2011
Available online 5 December 2011

Keywords:
Hydraulic fracture
Longitudinal fracture
Transverse fracture
Fracture initiation criteria
Inclined wellbores

ABSTRACT

The Hubbert and Willis (1957) [1] fracture criterion has been widely adopted to predict longitudinal fracture initiation in vertical or horizontal wellbores. Current transverse fracture criteria predict fracture by comparing the axial stress in the wellbore wall with the tensile strength of rock. It is shown in this paper that the axial stress is not a good predictor of transverse fracture initiation, because it remains constant during hydraulic pressurization. The magnitude of the most tensile principal stress in the wellbore wall should always be compared with the tensile strength of the rock to predict hydraulic fracture initiation based on elastic theory. Special cases have been found in which the most tensile principal stress reaches the tensile strength of the rock simultaneously at all point on the circumference of the wellbore. It is proposed that transverse fractures are initiated in those cases.

1. Introduction

Gas production of low permeability reservoirs is becoming increasingly important as conventional gas resources become depleted. The productivity of tight gas reservoirs is frequently enhanced artificially by the application of hydraulic pressure in the wellbore to cause fracturing of the surrounding rock. In the search for less accessible hydrocarbon resources, wells are typically going deeper and may also be deliberately inclined to the vertical (including horizontal wells). Successful completion of these deeper and inclined wells presents new challenges for the industry that must be faced on a daily basis. As new drilling techniques enable the exploitation of more complex and unconventional reservoirs, the theories that underlie the completion technologies must also advance, in order to optimize the stimulation and recovery of hydrocarbons through fracture initiation at multiple stages along the wellbore.

Hydraulic fracturing is one of the most popular well completion methods used to increase or restore the rate at which fluids, such as oil, gas or water, can be produced from a desired formation. The concept is quite simple because the creation of fractures increases the surface area of the reservoir exposed to the wellbore. Hydraulic fracturing is also used to estimate the in-situ stress in the surrounding rock (e.g., [2–5]).

A fundamental understanding of fracture initiation in arbitrarily inclined wellbores under various in-situ initial stress conditions is essential for the efficient and effective design of hydraulic fracture systems. For example, in thin, highly permeable formations, longitudinally fractured horizontal wells perform better than fractured vertical wells. Reservoirs, which possess natural fractures or create large differential stresses across horizontal sections, are more suitable for the successful placement of transverse fractures in horizontal wellbores.

Hubbert and Willis [1] developed the first realistic model relating the hydraulic fracturing test variables to the in-situ state of stress in rock. To avoid the need for determining tensile strength of rock, one of the most ambiguous rock mechanical properties (e.g. [6]), Bredehoeft et al. [7] suggested replacing the breakdown pressure with the fracture reopening pressure, obtained in subsequent pressurization cycles. Haimson and Fairhurst [8] invoked the theory of poroelasticity to incorporate the effect of the injection fluid permeation on the stress distribution around the wellbore.

Laboratory observations [9,10] and field observations [11] have demonstrated the initiation of transverse fractures and Fairhurst [12] has described the possibility of a fracture initiating as transverse and in the longitudinal direction. Weijers et al. [11] were unable to correlate the transverse fracture initiation pressure with that predicted by the Hubbert and Willis [1] criterion, which is valid only for predicting longitudinal fracture initiation in a vertical or horizontal well.

Ljunggren and Amadei [13] and Soliman [10] applied Hoek and Brown's [14] failure criterion to predict transverse fracture

* Corresponding author. Tel.: +61 2 49215118; fax: +61 2 49216991.
E-mail addresses: jinsong.huang@newcastle.edu.au (J. Huang), d.v.griffiths@mines.edu (D.V. Griffiths), sau-wai.wong@shell.com (S.-W. Wong).

1365-1609/$ - see front matter © 2011 Elsevier Ltd. All rights reserved.
doi:10.1016/j.ijrmms.2011.11.014

initiation; however, the Hoek–Brown criterion gives no information about fracture orientation. Another criterion of transverse fracture initiation (e.g., [15,16]) assumes that the axial stress on the wellbore wall exceeds the tensile strength of rock. The process of hydraulic fracturing consists essentially of injecting a fluid inside the wellbore and pressurizing it until the induced stresses exceeds the strength of the formation along some critical plane. Since axial stress remains constant during this process, it seems unlikely that it would be the cause of transverse fracture.

The basic equations describing the stress distribution around a horizontal, vertical and inclined wellbore may be derived from the solutions developed by Kirsch [17], Fairhurst [12] and Bradley [18], respectively. It is general believed that a fracture initiates when the maximum tensile stress induced at any point around the wellbore exceeds the tensile strength of the formation at that point. When this occurs, the resulting fracture on the wellbore wall will have an orientation that is perpendicular to the direction of the most tensile principal stress. The angle between the wellbore generatrix and the fracture orientation on the wellbore wall is called the trace angle (e.g., [19,20]), which can be observed by high-resolution electrical imaging technologies (e.g., [21]). It can also be used for inverse analysis in order to find the magnitude and orientation of in-situ stresses (e.g., [22,23]).

In this paper, elastic hydraulic fracturing theory is reviewed. It is shown that to predict facture initiation, the most tensile principal stress in the wellbore wall should always be compared with the tensile strength of the rock. For a vertical wellbore, this criterion reduces to the relation between breakdown pressure and in situ stress obtained by Hubbert and Willis [1]. A thorough investigation is conducted into the fracture initiation pressure and the resulting trace angle and angular position of the fracture on the wellbore circumference for arbitrarily inclined wellbores. Solutions cover normal faulting, reverse faulting and strike-slip faulting stress regions. It is found that fracture trace angles never reach ninety degrees. Special cases in which the most tensile principal stress reaches the tensile strength of rock at all point on the circumference of the wellbore have been found. It is proposed that transverse fractures are initiated in those cases

2. Theoretical development for stresses and hydraulic fracturing

Hydraulic fracturing consists of sealing off a short segment (typically 0.5–2 m) of a wellbore or borehole at the desired depth, injecting fluid into it at a rate sufficient to raise the hydraulic pressure quite rapidly (typically $0.1-1.0$ MPa/s), and bringing about hydraulic fracturing. The latter is achieved when the borehole fluid pressure reaches a critical level called breakdown pressure. At breakdown, the rock fractures in tension causing borehole fluid loss and hence a drop in pressure. When pumping is stopped, the hydraulic line to the testing interval remains in place. Following fracture, the pressure immediately decays, at first very quickly as the fluid chases the still extending fracturing tip, and then more slowly as the fracture closes, after which the only remaining fluid loss is due to seepage into the rock through the borehole wall. The "shut-in pressure" occurs at the transition between the fast and slow pressure decay and signifies the closure of the fracture.

In this section, elastic hydraulic fracturing theory is reviewed. The in situ principal stresses are assumed to be vertical and horizontal. The rock is assumed to be isotropic, homogeneous and linearly elastic. The ambient pore pressure in the rock is assumed to remain constant during the test. However, the method presented can easily be extended to cases where fluid penetrates into surrounding rock, in which case poro-elastic theory must be adopted. Aadnoy and Belayneh [24] showed that elastic model under-predicted the fracture pressure for non-penetrating cases. For more accurate modeling, an elastoplastic model should be used (e.g., [25]).

Referring to Fig. 1 and assuming a compression positive convention, let σ_v, σ_H and σ_h ($\sigma_H > \sigma_h$) be the initial in situ vertical and horizontal principal stresses, respectively (σ_H is the most compressive horizontal principal stress). Let the origin of the principal stress axes lie at the center of the top of the inclined wellbore shown in the figure. Consider the local coordinates of the wellbore (x,y,z) with the same origin, where the x-axis passes through the highest point of the circumference and the z-axis passes down the longitudinal axis. The wellbore azimuth φ is the horizontal angle between the vertical plane containing the σ_h-axis and the vertical plane containing the x-axis, measured counterclockwise as viewed down the σ_v-axis looking towards the origin. The wellbore inclination γ is the angle between the σ_v-axis and the z-axis measured clockwise as viewed down the y-axis looking towards the origin.

The geometry of fractures initiated along an arbitrarily inclined wellbore is strongly dependent on in situ stresses (σ_v, σ_H and σ_h), wellbore azimuth (φ) and inclination (γ). The fracture trace angle β between the fracture trace and wellbore generatrix is measured in a clockwise direction when looking outwards from the wellbore axis.

For an arbitrarily oriented wellbore, the rotation of the stress tensor from the in situ coordinate system to a local wellbore coordinate system (Fig. 1) is given by

$$\begin{Bmatrix} \sigma_x \\ \sigma_y \\ \sigma_z \\ \tau_{xy} \\ \tau_{yz} \\ \tau_{zx} \end{Bmatrix} = \begin{bmatrix} \cos^2\varphi\cos^2\gamma & \sin^2\varphi\cos^2\gamma & \sin^2\gamma \\ \sin^2\varphi & \cos^2\varphi & 0 \\ \cos^2\varphi\sin^2\gamma & \sin^2\varphi\sin^2\gamma & \cos^2\gamma \\ -\sin\varphi\cos\varphi\cos\gamma & \sin\varphi\cos\varphi\cos\gamma & 0 \\ \sin\varphi\cos\varphi\sin\gamma & -\sin\varphi\cos\varphi\sin\gamma & 0 \\ -\cos^2\varphi\sin\gamma\cos\gamma & -\sin^2\varphi\sin\gamma\cos\gamma & \sin\gamma\cos\gamma \end{bmatrix} \begin{Bmatrix} \sigma_h \\ \sigma_H \\ \sigma_v \end{Bmatrix} \tag{1}$$

Let θ be the angle measured counterclockwise starting at $\theta=0$ on the x-axis as viewed down the z-axis looking towards the origin.

Stresses at the wellbore wall are (e.g., [18])

$$\begin{aligned} \sigma_r &= P_w \\ \sigma_\theta &= \sigma_x+\sigma_y-2(\sigma_x-\sigma_y)\cos(2\theta)-4\tau_{xy}\sin(2\theta)-P_w \\ \sigma_\zeta &= \sigma_z-\upsilon\{2(\sigma_x-\sigma_y)\cos(2\theta)+4\tau_{xy}\sin(2\theta)\} \\ \tau_{r\theta} &= 0 \\ \tau_{\theta\zeta} &= -2\tau_{xz}\sin\theta+2\tau_{yz}\cos\theta \\ \tau_{\zeta r} &= 0 \end{aligned} \tag{2}$$

where P_w is the compressive applied wellbore pressure, and υ is Poisson's ratio.

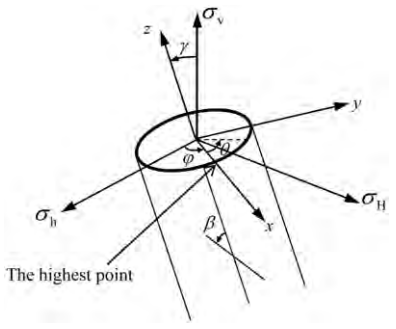

Fig. 1. Wellbore configuration.

Thus the effective stress tensor is

$$\sigma' = \begin{bmatrix} \sigma'_r & 0 & 0 \\ 0 & \sigma'_\theta & \tau_{\theta\zeta} \\ 0 & \tau_{\theta\zeta} & \sigma'_\zeta \end{bmatrix} \tag{3}$$

where $\sigma'_r = \sigma_r - P_0$, $\sigma'_\theta = \sigma_\theta - P_0$, $\sigma'_\zeta = \sigma_\zeta - P_0$, and P_0 is the pore pressure.

The effective principal stresses at the wellbore can be found as the eigenvalues of the effective stress tensor, thus

$$\begin{aligned} \sigma'_1 &= \sigma'_r \\ \sigma'_2 &= \frac{(\sigma'_\theta + \sigma'_\zeta) + \sqrt{(\sigma'_\theta - \sigma'_\zeta)^2 + 4\tau^2_{\theta\zeta}}}{2} \\ \sigma'_3 &= \frac{(\sigma'_\theta + \sigma'_\zeta) - \sqrt{(\sigma'_\theta - \sigma'_\zeta)^2 + 4\tau^2_{\theta\zeta}}}{2} \end{aligned} \tag{4}$$

with corresponding eigenvectors given as

$$\begin{aligned} \vec{\sigma}'_1 &= \begin{pmatrix} 1 \\ 0 \\ 0 \end{pmatrix} \\ \vec{\sigma}'_2 &= \frac{1}{(\sigma'_\theta - \sigma'_2)^2 + 4\tau^2_{\theta\zeta}} \begin{pmatrix} 0 \\ \tau_{\theta\zeta} \\ -(\sigma'_\theta - \sigma'_2) \end{pmatrix} \\ \vec{\sigma}'_3 &= \frac{1}{(\sigma'_\theta - \sigma'_3)^2 + 4\tau^2_{\theta\zeta}} \begin{pmatrix} 0 \\ \tau_{\theta\zeta} \\ -(\sigma'_\theta - \sigma'_3) \end{pmatrix} \end{aligned} \tag{5}$$

Assuming that σ'_3 is the smallest, and hence the most tensile principal stress, tensile failure occurs when

$$\sigma'_3 = \sigma_t \tag{6}$$

where σ_t is the tensile strength of rock.

Since $\sigma_r = P_w$ is one of the principal stresses, we get

$$\tan(2\beta) = \frac{2\tau_{\theta\zeta}}{\sigma'_\theta - \sigma'_\zeta} \tag{7}$$

Furthermore

$$\frac{\partial \sigma'_3}{\partial \theta} = 0 \tag{8}$$

where

$$\begin{aligned} \frac{\partial \sigma'_3}{\partial \theta} &= \frac{1}{2}\left(\frac{\partial \sigma'_\theta}{\partial \theta} + \frac{\partial \sigma'_z}{\partial \theta}\right) - \frac{1}{4}((\sigma'_\theta - \sigma'_\zeta)^2 + 4\tau^2_{\theta\zeta})^{-(1/2)} \\ &\quad \times \left(2(\sigma'_\theta - \sigma'_\zeta)\left(\frac{\partial \sigma'_\theta}{\partial \theta} - \frac{\partial \sigma'_\zeta}{\partial \theta}\right) + 8\tau_{\theta\zeta}\frac{\partial \tau_{\theta\zeta}}{\partial \theta}\right) \end{aligned}$$

$$\frac{\partial \sigma'_\theta}{\partial \theta} = 4(\sigma_x - \sigma_y)\sin(2\theta) - 8\tau_{xy}\cos(2\theta)$$

$$\frac{\partial \sigma'_\zeta}{\partial \theta} = 4\upsilon(\sigma_x - \sigma_y)\sin(2\theta) - 8\upsilon\tau_{xy}\cos(2\theta)$$

$$\frac{\partial \tau_{\theta\zeta}}{\partial \theta} = -2\tau_{xz}\cos\theta - 2\tau_{yz}\sin\theta$$

For σ'_3 to be a minimum

$$\frac{\partial^2 \sigma'_3}{\partial \theta^2} > 0 \tag{9}$$

and by solving Eq. (8), the circumferential angle θ_m where fracture is initiated can be obtained.

It should be noted that β depends on the signs of $\tau_{\theta\zeta}$ and $\sigma'_\theta - \sigma'_\zeta$ and Table 1 shows how to determine β from Eq. (7).

Table 1
Fracture trace angle determination.

$\tau_{\theta\zeta} > 0, \sigma'_\theta > \sigma'_\zeta$	$0^\circ < \beta < 45^\circ$
$\tau_{\theta\zeta} < 0, \sigma'_\theta > \sigma'_\zeta$	$-45^\circ < \beta < 0^\circ$
$\tau_{\theta\zeta} > 0, \sigma'_\theta < \sigma'_\zeta$	$45^\circ < \beta < 90^\circ$
$\tau_{\theta\zeta} < 0, \sigma'_\theta < \sigma'_\zeta$	$-90^\circ < \beta < -45^\circ$
$\tau_{\theta\zeta} = 0, \sigma'_\theta > \sigma'_\zeta$	$\beta = 0^\circ$
$\tau_{\theta\zeta} = 0, \sigma'_\theta < \sigma'_\zeta$	$\beta = 90^\circ$

3. Observations on hydraulic fracture criteria

Knowing in-situ stresses σ_H and σ_h, wellbore inclination γ and azimuth φ, breakdown pressure P_w and the circumferential angle θ_m, the location of fracture initiation can be obtained by solving simultaneous nonlinear Eqs. (1)–(4), (6) and (8). Any conventional numerical nonlinear equation solver (e.g. Newton–Raphson) can be used. Note that Eq. (9) should be satisfied to ensure σ'_3 is a minimum.

For a vertical wellbore ($\gamma = 0^\circ$), explicit analytical solutions can be obtained. Substitution of $\gamma = 0^\circ$ into Eq. (1) gives

$$\begin{aligned} \sigma_x &= \sigma_h \cos^2\varphi + \sigma_H \sin^2\varphi \\ \sigma_y &= \sigma_h \sin^2\varphi + \sigma_H \cos^2\varphi \\ \sigma_z &= \sigma_v \\ \tau_{xy} &= (\sigma_H - \sigma_h)\sin\varphi\cos\varphi \\ \tau_{yz} &= 0 \\ \tau_{zx} &= 0 \end{aligned} \tag{10}$$

and substitution of Eq. (10) into Eqs. (2) and (3) gives

$$\begin{aligned} \sigma'_r &= P_w - P_0 \\ \sigma'_\theta &= \sigma_H + \sigma_h - 2(\sigma_h - \sigma_H)\cos(2\varphi)\cos(2\theta) \\ &\quad -2(\sigma_H - \sigma_h)\sin(2\varphi)\sin(2\theta) - P_w - P_0 \\ \sigma'_\zeta &= \sigma_v - \upsilon\{2(\sigma_h - \sigma_H)\cos(2\varphi)\cos(2\theta) \\ &\quad +2(\sigma_H - \sigma_h)\sin(2\varphi)\sin(2\theta)\} - P_0 \\ \tau_{r\theta} &= 0 \\ \tau_{\theta\zeta} &= 0 \\ \tau_{\zeta r} &= 0 \end{aligned} \tag{11}$$

It can be seen from Eq. (11) that all shear stresses on the wellbore wall are zero since $\sigma'_r, \sigma'_\theta$ and σ'_ζ are principal stresses. It can also be noted that σ'_ζ is independent of P_w. As P_w increases, σ'_ζ remains constant, but σ'_θ decreases. It follows that σ'_θ will always be smaller than σ'_ζ when hydraulic fractures are initiated and will be the most tensile principal stress ($\sigma'_3 = \sigma'_\theta$).

The circumferential angle θ_m where fracture is initiated can be obtained by solving

$$\frac{\partial \sigma'_3}{\partial \theta} = \frac{\partial \sigma'_\theta}{\partial \theta} = 0 \tag{12}$$

where from Eq. (11)

$$\frac{\partial \sigma'_\theta}{\partial \theta} = 4(\sigma_h - \sigma_H)\cos(2\varphi)\sin(2\theta) + 4(\sigma_h - \sigma_H)\sin(2\varphi)\cos(2\theta) \tag{13}$$

Substituting Eq. (13) into Eq. (12) gives

$$\tan(2\theta_m) = -\tan(2\varphi) \tag{14}$$

or $\theta_m = -\varphi$, which is one of the conditions that $\sigma'_\theta (= \sigma'_3)$ reaches a minimum. Another condition that needs to be checked is inequality (9). Taking the derivative of Eq. (13), Eq. (9) can be written as

$$\sin(2\varphi)\sin(2\theta_m) > \cos(2\varphi)\cos(2\theta_m) \tag{15}$$

Since $0^\circ \le \varphi \le 90^\circ$, then $\sin(2\varphi)\sin(2\theta_m) \le 0$ and $\cos(2\varphi)\cos(2\theta_m) \ge 0$. The only two solutions that satisfy Eq. (14) and inequality (15) are $\varphi = 90^\circ$, $\theta_m = 0^\circ$ and $\varphi = 0^\circ$, $\theta = 90^\circ$. For both

these cases, fracture is initiated in the direction of σ_H as shown in Fig. 1.

Substitution of $\varphi=90^\circ$ and $\theta_m=0^\circ$ or $\varphi=0^\circ$ and $\theta_m=90^\circ$ into Eq. (11) gives

$$\sigma'_\theta=3\sigma_h-\sigma_H-P_w-P_0 \tag{16}$$

Since $\sigma'_3=\sigma'_\theta$, from Eqs. (6) and (16),

$$P_w=3\sigma_h-\sigma_H-P_0+\sigma_t \tag{17}$$

Eq. (17) is the hydraulic fracture initiation criterion for vertical wellbore obtained by Hubbert and Willis [1].

Because $\tau_{\theta\zeta}=0$ and $\sigma'_\theta<\sigma'_\zeta$, it can been seen from Table 1 that hydraulic fractures are always vertical and $\beta=0$ for vertical wellbores.

Some investigators (e.g., Hossain et al. [15], Nelson et al. [16]) have checked whether σ'_ζ exceeds the tensile strength of rock and the following two criteria must be met to facilitate formation of a transverse hydraulic fracture:

1. The axial wellbore stress must be smaller than or equal to tensile strength of rock ($\sigma'_\zeta\le\sigma_t$) permitting the development of transverse fractures.
2. The axial wellbore stress must be smaller than or equal to the circumferential stress ($\sigma'_\zeta\le\sigma'_\theta$) precluding the formation of a longitudinal fracture (assuming transverse fractures do not co-exist with the longitudinal fractures).

Ljunggren and Amadei [13] and Soliman [10] applied Hoek and Brown's [14] failure criterion to predict transverse fracture initiation. The following two conditions were assumed

$$\sigma'_\zeta\le\sigma'_\theta\le\sigma'_r \tag{18}$$

and

$$\sigma'_r=\sigma'_\zeta+\sqrt{m\sigma_t\sigma'_\zeta+\sigma_t^2} \tag{19}$$

where m is an empirical constant that depends on the properties of the rock type.

Since axial stress σ'_ζ remains constant during hydraulic pressurization, the condition $\sigma'_\zeta\le\sigma'_\theta$ cannot be satisfied. Moreover, the Hoek and Brown [14] failure criterion gives no information about fracture orientation and thus cannot be used for the determination of whether a transverse fracture is initiated.

It can be shown however, that transverse fracture can be initiated if σ'_3 at all points on the circumference of the wellbore reach σ_t at the same time. For a vertical wellbore, if $\sigma_h=\sigma_H$, from Eq. (11)

$$\begin{aligned}&\sigma'_r=P_w-P_0\\&\sigma'_\theta=2\sigma_{\mathrm{H}}-P_w-P_0=2\sigma_{\mathrm{h}}-P_w-P_0\\&\sigma'_\zeta=\sigma_{\mathrm{v}}-P_0\\&\tau_{r\theta}=0\\&\tau_{\theta\zeta}=0\\&\tau_{\zeta r}=0\end{aligned} \tag{20}$$

It can be seen from Eq. (20), σ'_θ is the most tensile principal stress and independent of θ in this case. As P_w increases, σ'_θ reaches σ_t and a transverse fracture will be initiated. The breakdown pressure is then given by $P_w=2\sigma_H-P_0+\sigma_t$.

For deviated wellbores, under certain in situ stress conditions, there may be some cases that the most tensile principal stress is independent of θ to facilitate transverse hydraulic fractures. Unfortunately, simultaneous nonlinear Eqs. (1)–(4), (6) and (8) need to be solved for deviated wellbores to obtain the most tensile principal stress distributions along the circumference of wellbore. To investigate breakdown pressure, location and orientation of hydraulic fracture initiation of deviated wellbores, thorough parametric studies are conducted in the following section.

4. Parametric studies of hydraulic fracturing

With known in-situ stress conditions, and by changing the wellbore inclination in the range $0^\circ\le\gamma\le90^\circ$, Eqs. (1)–(4), (6) and (8) can be used to give the angular position of fracture θ_m , and the breakdown pressure P_w. Finally, the fracture trace angle β can then be determined by Eq. (7).

The results from this study are presented in the form of non-dimensional charts in Figs. 2–21. The breakdown pressure P_w is normalized with respect to σ_v, and the ratios of in-situ stresses σ_H/σ_v and σ_H/σ_h, are varied to cover normal faulting ($\sigma_v>\sigma_H>\sigma_h$) , reverse faulting ($\sigma_H>\sigma_h>\sigma_v$) and strike-slip faulting ($\sigma_H>\sigma_v>\sigma_h$). For simplicity, $P_0=0$, $\sigma_t=0.0$ and $\upsilon=0.0$.

Hossain et al. [15] has previously presented parametric studies of breakdown pressure and the orientation and location of fractures on the wellbore wall. The present parametric studies closely follow those presented by Hossain et al. [15], however, but go further, to give additional solutions for the angular location (θ_m) and trace angle (β) of fracture initiation on the wellbore wall. The charts were obtained using one degree increment of γ. The charts were drawn without smoothing to show clearly the optimum wellbore orientation as observed by Hossain et al. [15], which requires minimum fluid pressure for fracture

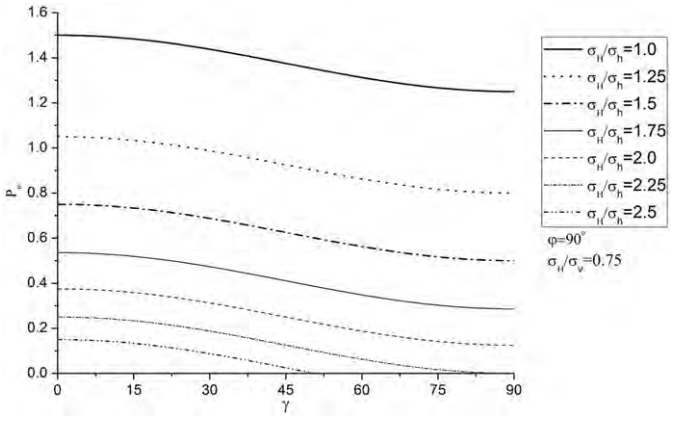

Fig. 2. Fracture initiation pressure P_w for wellbore deviation $\varphi=90^o$ and different inclination γ under moderate normal faulting stress condition. (The corresponding angular position of fracture θ_m and fracture trace angle β are all zero and not presented.)

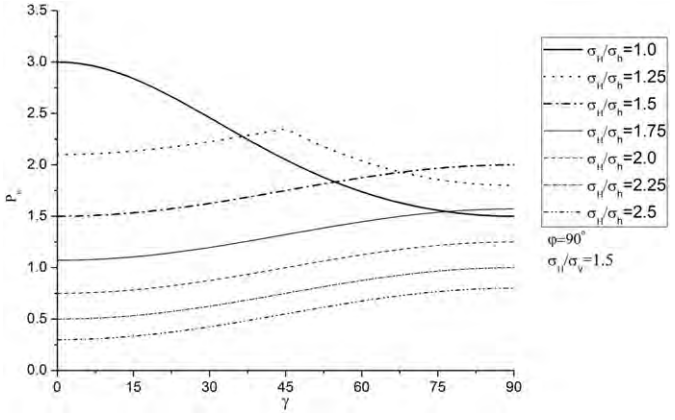

Fig. 3. Fracture initiation pressure P_w for wellbore deviation $\varphi=90^o$ and different inclination γ under reverse faulting and strike slip faulting stress condition.

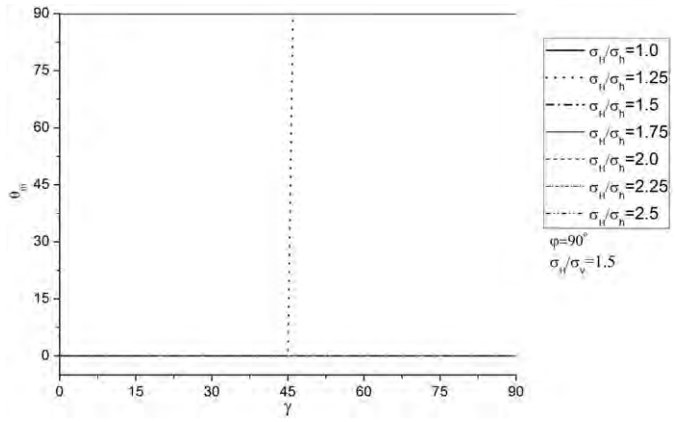

Fig. 4. Angular position of fracture θ_m for wellbore deviation $\varphi=90^o$ and different inclination γ under reverse faulting and strike slip faulting stress condition.

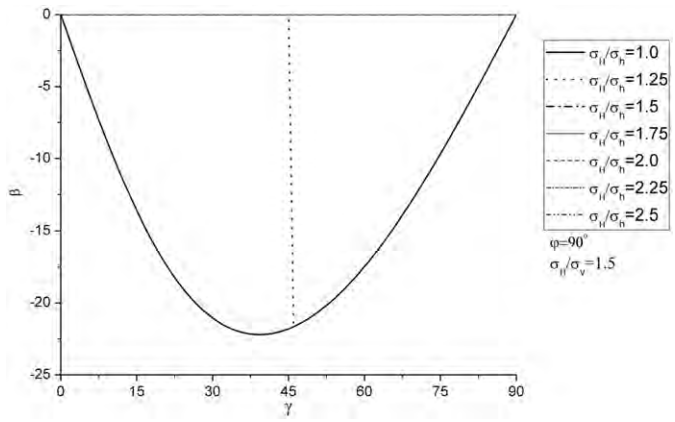

Fig. 5. Fracture trace angle β for wellbore deviation $\varphi=90^o$ and different inclination γ under reverse faulting and strike slip faulting stress condition.

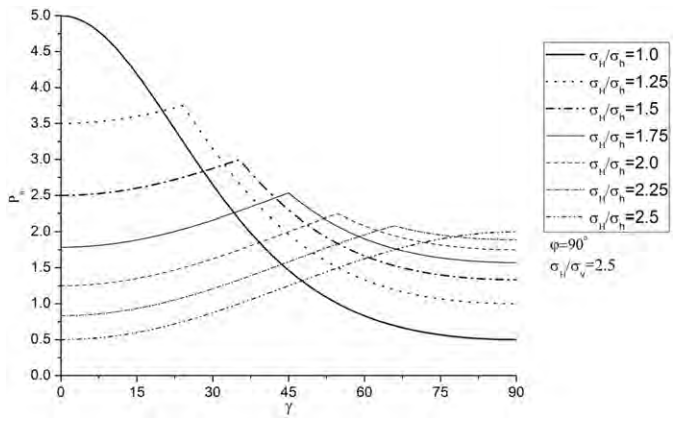

Fig. 6. Fracture initiation pressure P_w for wellbore deviation $\varphi=90^o$ and different inclination γ under reverse faulting stress condition.

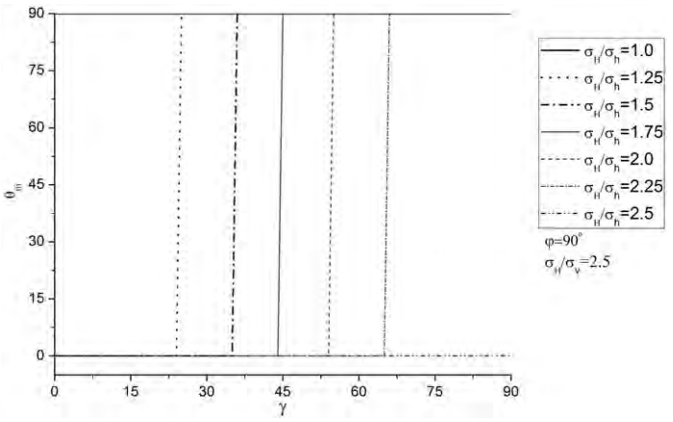

Fig. 7. Angular position of fracture θ_m for wellbore deviation $\varphi=90^o$ and different inclination γ under reverse faulting stress condition.

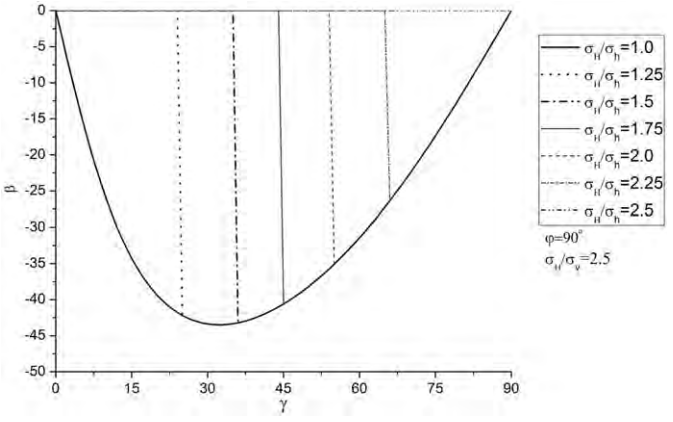

Fig. 8. Fracture trace angle β for wellbore deviation $\varphi=90^o$ and different inclination γ under reverse faulting stress condition.

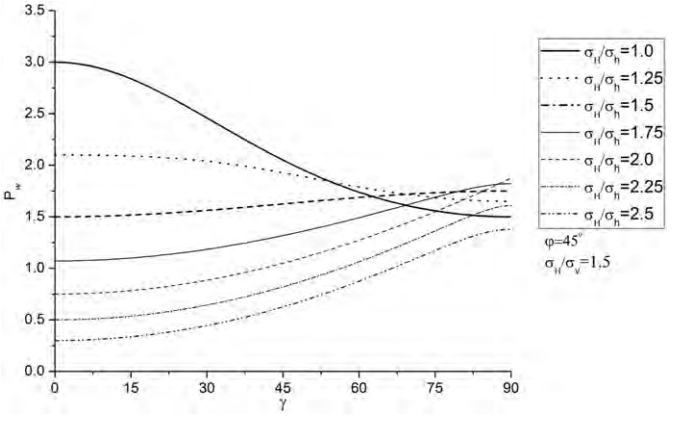

Fig. 9. Fracture initiation pressure P_w for wellbore deviation $\varphi=45^o$ and different inclination γ under reverse faulting and strike slip faulting stress condition.

initiation. Moreover, analytical relations between breakdown pressure and in situ stress are provided whenever possible (e.g., Eqs. (22), (23), (29), (30), (32), (34)) in the following. Yew and Li [26] presented similar charts for a particular in situ stress condition. The charts presented in this paper cover all in-situ stress conditions and are useful for the design of hydraulic fracture systems such as perforation, and give guidance as to whether a hydraulic fracture will be deviated, longitudinal or transverse. Based on elasticity theory, Huang et al. [23] proposed a method to determine in situ stress from inversion of hydraulic fracturing data. The charts presented are also useful for determining an initial guess to use with the method by Huang et al. [23].

4.1. *Wellbore azimuth* $\varphi=90^\circ$

In this special case Eq. (2) can be written in terms of the in-situ stress

$\sigma_r = P_w$

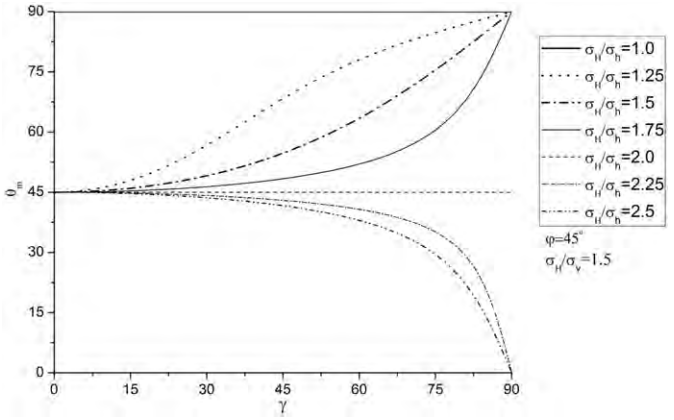

Fig. 10. Angular position of fracture θ_m for wellbore deviation $\varphi=45°$ and different inclination γ under reverse faulting and strike slip faulting stress condition.

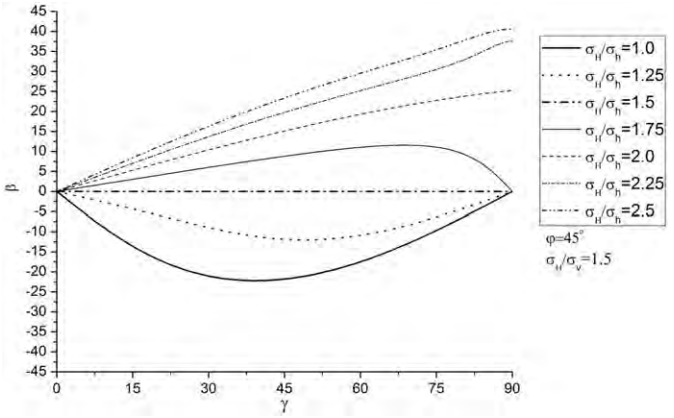

Fig. 11. Fracture trace angle β for wellbore deviation $\varphi=45°$ and different inclination γ under reverse faulting and strike slip faulting stress condition.

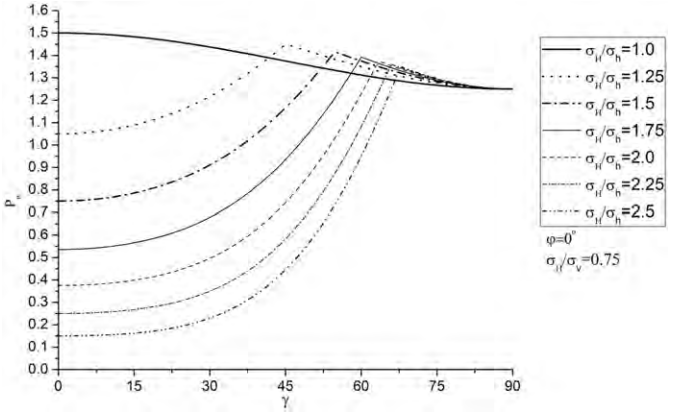

Fig. 12. Fracture initiation pressure P_w for wellbore deviation $\varphi=0°$ and different inclination γ under moderate normal faulting stress condition.

$$\sigma_\theta = \sigma_H \cos^2\gamma + \sigma_v \sin^2\gamma + \sigma_h - 2(\sigma_H \cos^2\gamma + \sigma_v \sin^2\gamma - \sigma_h)\cos(2\theta) - P_w$$

$$\sigma_\zeta = \sigma_H \sin^2\gamma + \sigma_v \cos^2\gamma - 2\upsilon(\sigma_H \cos^2\gamma + \sigma_v \sin^2\gamma - \sigma_h)\cos(2\theta)$$

$$\tau_{r\theta} = 0$$

$$\tau_{\theta\zeta} = 2(\sigma_v - \sigma_H)\cos\gamma \sin\gamma \sin\theta$$

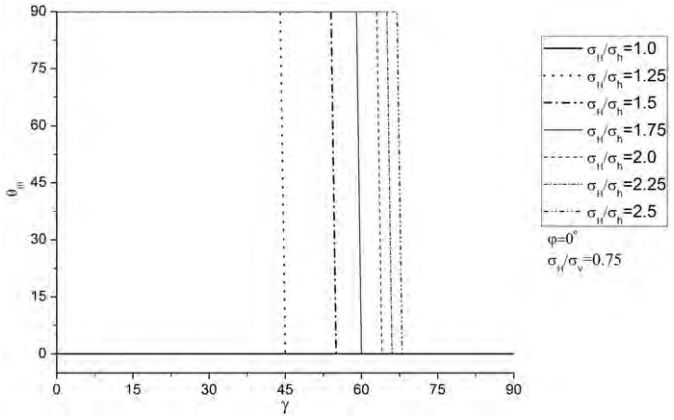

Fig. 13. Angular position of fracture θ_m for wellbore deviation $\varphi=0°$ and different inclination γ under moderate normal faulting stress condition.

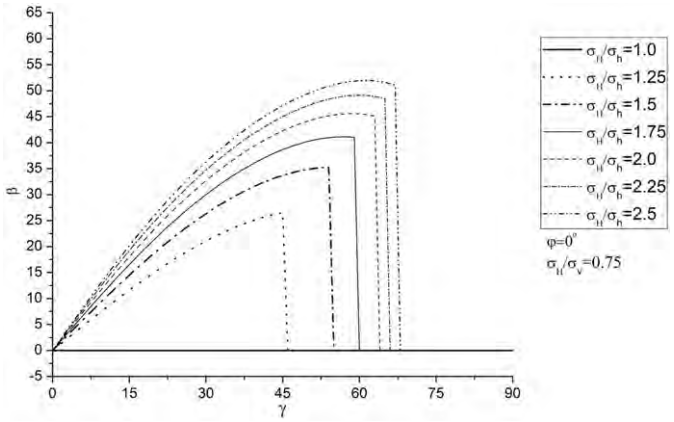

Fig. 14. Fracture trace angle β for wellbore deviation $\varphi=0°$ and different inclination γ under moderate normal faulting stress condition.

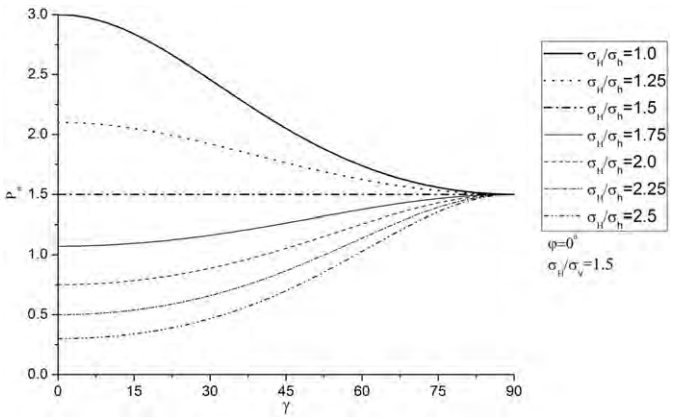

Fig. 15. Fracture initiation pressure P_w for wellbore deviation $\varphi=0°$ and different inclination γ under reverse faulting and strike-slip stress condition. (The corresponding angular position of fracture θ_m are 90 degrees and not presented.).

$$\tau_{\zeta r} = 0 \tag{21}$$

The shear stress $\tau_{\theta\zeta}$ vanishes when $\theta=0$ or $\theta=180^\circ$, which implies that σ_θ at these points is a principal stress. Assuming $\sigma_\theta=\sigma_t$ and $\theta_m=0^\circ$ or 180°, Haimson [4] suggested using the following equation to obtain σ_H

$$\sigma_H = \frac{3\sigma_h - \sigma_v \sin^2\gamma - P_w}{\cos^2\gamma} \tag{22}$$

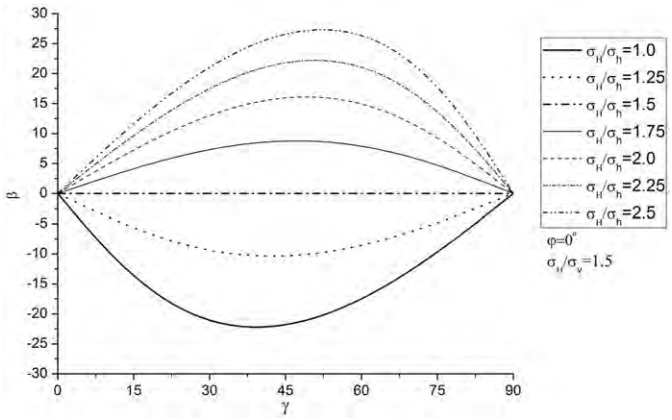

Fig. 16. Fracture trace angle β for wellbore deviation $\varphi=0^{o}$ and different inclination γ under reverse faulting and strike-slip stress condition.

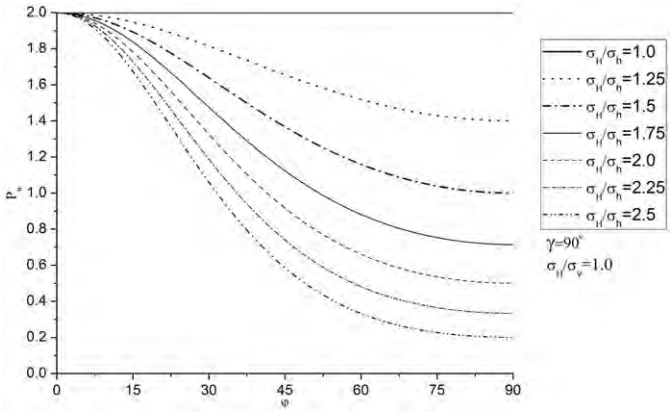

Fig. 17. Fracture initiation pressure P_w for horizontal wellbore and different azimuth φ under normal faulting and strike slip stress conditions. (The corresponding angular position of fracture θ_m is zero and not presented.).

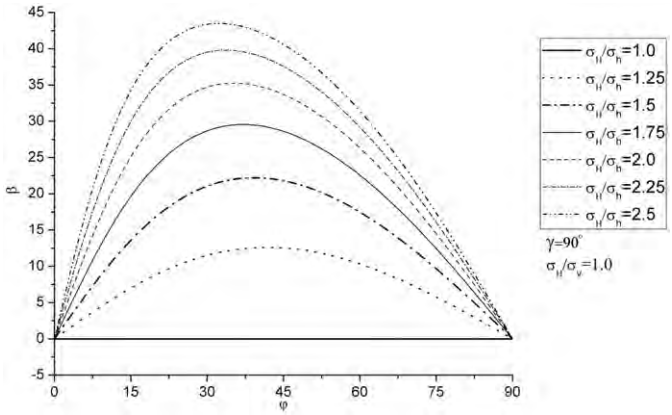

Fig. 18. Fracture trace angle β for horizontal wellbore and different azimuth φ under normal faulting and strike slip stress conditions.

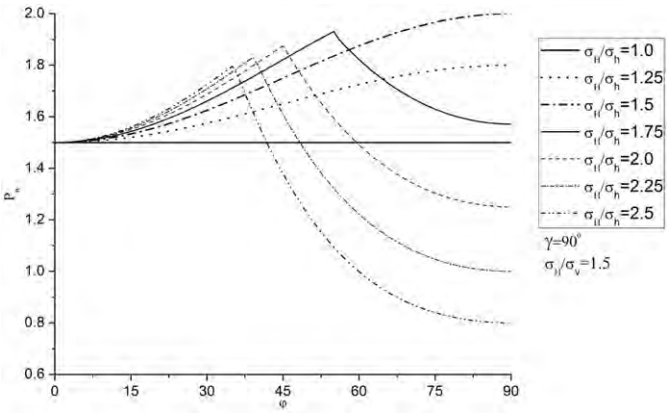

Fig. 19. Fracture initiation pressure P_w for horizontal wellbore and different azimuth φ under reverse faulting and strike slip stress conditions.

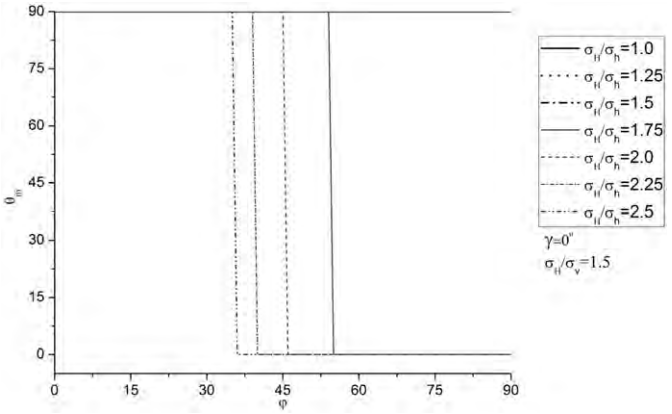

Fig. 20. Angular position of fracture θ_m for horizontal wellbore and different azimuth φ under reverse faulting and strike slip stress conditions.

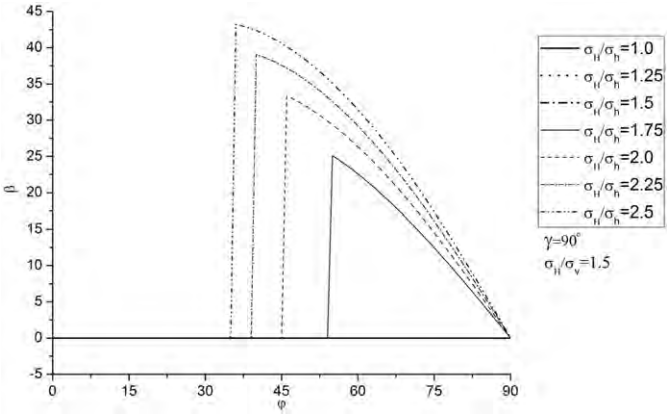

Fig. 21. Fracture trace angle β for horizontal wellbore and different azimuth φ under reverse faulting and strike slip stress conditions.

Although σ_θ becomes a principal stress at $\theta=0^\circ$ or $\theta=180^\circ$, it is not necessarily the most tensile principal stress compared with other locations around the circumference from $\theta=0^\circ$ to 360°. Based on the results shown in Figs. 2–8, under normal faulting stress condition, the angular position of fracture θ_m is zero. However, for reverse faulting and strike slip faulting stress conditions, the angular position of fracture θ_m could be at 90° (Figs. 4 and 7) when the wellbore inclination is high. The relation between the breakdown pressure and σ_H is nonlinear as indicated by

$$P_w = 3\sigma_H\cos^2\gamma + 3\sigma_v\sin^2\gamma - \sigma_h - \frac{4(\sigma_v-\sigma_H)^2\cos^2\gamma\sin^2\gamma}{\sigma_H\sin^2\gamma+\sigma_v\cos^2\gamma} \quad (23)$$

Under reverse faulting and strike slip faulting stress condition when the wellbore inclination is high, Eq. (23) must be used for inversion of σ_H from breakdown pressure. The fracture trace angle β is not zero and independent of σ_h (Figs. 5 and 8) when $\theta_m=90^\circ$. By setting $\theta=90^\circ$, $\upsilon=0.0$ and $\sigma_t=0.0$ in Eq. (21) and solving for

P_w, Eq. (7) gives the following equation:

$$\tan\beta = \frac{2((\sigma_H-\sigma_v)\cos^2\gamma-\sigma_H)(\sigma_H-\sigma_v)\sin\gamma\cos\gamma}{(\sigma_H\sin^2\gamma+\sigma_v\cos^2\gamma)^2-2(\sigma_H-\sigma_v)\sin\gamma\cos\gamma} \quad (24)$$

which demonstrates that the fracture trace angle β is independent of σ_h.

It can be seen from Figs. 3 and 6 that under reverse faulting stress condition, there is a critical inclination at which the breakdown pressure is maximum. This is because the most tensile principal stress initially remains constant at the value of tensile strength of rock while the intermediate principal stress increases with inclination. At a critical point, the two principal stress are both equal to σ_t. With further rotation, the intermediate principal stress decreases and the most tensile principal stress remains constant at the value of σ_t. Details can be found in [26].

4.2. Wellbore azimuth axis $\varphi=45^o$

This is the most general case for which no analytical solutions can be obtained. A special case has been found when transverse fracture is initiated in a horizontal wellbore occurs when, $\sigma_H/\sigma_v=1.5$ and $\sigma_H/\sigma_h=2$ (referring to Figs. 9–11).

Assume $\sigma_v=1.0$, solving Eqs. (1)–(4), (6) and (8) gives $P_w=1.875$.

According to Eq. (2)

$$\begin{aligned}&\sigma_\theta = 0.25+0.25\cos(2\theta)\\ &\sigma_\zeta = 1.125\\ &\tau_{\theta\zeta} = 0.75\cos\theta\end{aligned} \quad (25)$$

From Eq. (25)

$$\sigma_\theta\sigma_\zeta = 0.28125(1+\cos(2\theta)) = 0.5625\cos^2\theta \quad (26)$$

thus

$$\sigma_\theta\sigma_\zeta = \tau_{\theta\zeta}^2 \quad (27)$$

Substituting Eq. (27) into Eq. (4) indicates that σ_3 remains zero regardless of the value of θ.

Although σ_θ, σ_ζ and $\tau_{\theta\zeta}$ are all functions of θ, the most tensile principal stress remains zero everywhere along the circumference of wellbore so a transverse fracture will be initiated.

4.3. Wellbore azimuth $\varphi=0^\circ$

In this special case Eq. (2) can be represented in terms of the in-situ stress

$$\begin{aligned}&\sigma_r = P_w\\ &\sigma_\theta = \sigma_h\cos^2\gamma+\sigma_v\sin^2\gamma+\sigma_H\\ &\quad -2(\sigma_h\cos^2\gamma+\sigma_v\sin^2\gamma-\sigma_H)\cos(2\theta)-P_w\\ &\sigma_\zeta = \sigma_h\sin^2\gamma+\sigma_v\cos^2\gamma\\ &\quad -2\upsilon(\sigma_h\cos^2\gamma+\sigma_v\sin^2\gamma-\sigma_H)\cos(2\theta)\\ &\tau_{r\theta} = 0\\ &\tau_{\theta\zeta} = 2(\sigma_v-\sigma_h)\cos\gamma\sin\gamma\sin\theta\\ &\tau_{\zeta r} = 0\end{aligned} \quad (28)$$

Based on the results presented in Figs. 12–16, for reverse faulting and strike slip faulting stress condition, the angular position of fracture θ_m is always 90°.

Assuming $\upsilon=0$, $\sigma_t=0$ and $P_0=0$

$$\sigma_H = 3\sigma_h\cos^2\gamma+3\sigma_v\sin^2\gamma-\frac{4(\sigma_v-\sigma_h)^2\cos^2\gamma\sin^2\gamma}{\sigma_h\sin^2\gamma+\sigma_v\cos^2\gamma}3\sigma_h\cos^2\gamma+3\sigma_v\sin^2\gamma-P_w \quad (29)$$

Eq. (29) can be used to estimate σ_H when σ_h has been estimated by a "leak-off" test in a vertical wellbore of the same field. It should be noted that Eq. (29) does not imply that σ_θ is the most tensile principal stress since $\tau_{\theta\zeta}$ does not vanish at $\theta=90^\circ$. Fig. 16 confirms that the fracture trace angles are not equal to zero.

It should be emphasized that Eq. (29) is applicable only to reverse faulting and strike slip faulting stress conditions. Under normal faulting stress condition, the angular position of fracture θ_m could be 0° (Fig. 13) when the wellbore inclination is high. The breakdown pressure can be obtained from

$$P_w = 3\sigma_H-\sigma_h\cos^2\gamma-\sigma_v\sin^2\gamma \quad (30)$$

As before, there is a critical inclination at which the breakdown pressure reaches a maximum (Fig. 12). The explanation is the same as the previous case when the wellbore axis lay along the σ_H-axis under reverse faulting stress condition.

4.4. Horizontal wells ($\gamma=90^\circ$)

For horizontal wells, Eq. (2) can be represented in terms of the in-situ stress

$$\begin{aligned}&\sigma_r = P_w\\ &\sigma_\theta = \sigma_H\cos^2\varphi+\sigma_h\sin^2\varphi+\sigma_v\\ &\quad -2(\sigma_v-\sigma_H\cos^2\varphi-\sigma_h\sin^2\varphi)\cos(2\theta)-P_w\\ &\sigma_\zeta = \sigma_H\sin^2\varphi+\sigma_h\cos^2\varphi\\ &\quad -2\upsilon(\sigma_v-\sigma_H\cos^2\varphi-\sigma_h\sin^2\varphi-\sigma_H)\cos(2\theta)\\ &\tau_{r\theta} = 0\\ &\tau_{\theta\zeta} = 2(\sigma_h-\sigma_H)\cos\varphi\sin\varphi\cos\theta\\ &\tau_{\zeta r} = 0\end{aligned} \quad (31)$$

Figs. 17–21 present breakdown pressures P_w, angular position of fracture θ_m and fracture trace angle β of horizontal wellbores with different values of azimuth φ under different in-situ stress conditions.

The corresponding angular positions of fracture θ_m for Fig. 17 are all zero and not presented. Substituting $\theta=0^\circ$ into Eq. (31), the breakdown pressure can be explicitly expressed as

$$P_w = 3\sigma_H\cos^2\varphi+3\sigma_h\sin^2\varphi-\sigma_v-\frac{4(\sigma_h-\sigma_H)^2\cos^2\varphi\sin^2\varphi}{\sigma_H\sin^2\varphi+\sigma_h\cos^2\varphi} \quad (32)$$

It can be seen from Fig. 17 that the breakdown pressure decreases as φ increases under normal faulting stress conditions. A wellbore oriented along σ_h under normal faulting stress condition requires the maximum pressure for fracture initiation. This pressure can be found analytically by substituting $\varphi=0^\circ$ into Eq. (32):

$$P_w = 3\sigma_H-\sigma_v \quad (33)$$

which is independent of σ_h.

Similarly a wellbore along σ_H under normal faulting stress condition requires the minimum pressure for fracture initiation, which can be found by

$$P_w = 3\sigma_h-\sigma_v \quad (34)$$

It can be seen from Fig. 20 that the corresponding angular position of fracture θ_m for reverse faulting stress condition are all ninety degrees. Substituting $\theta=90^\circ$ into Eq. (31), the breakdown pressure can be explicitly written as

$$P_w = 3\sigma_v-\sigma_H\cos^2\varphi-\sigma_h\sin^2\varphi \quad (35)$$

It can be seen from Fig. 19 that a wellbore oriented along σ_h under reverse faulting stress condition requires the minimum pressure for fracture initiation. This pressure can be found analytically by substituting $\varphi=0^\circ$ into Eq. (35):

$$P_w = 3\sigma_v-\sigma_H \quad (36)$$

which is independent of σ_h.

Similarly a wellbore along σ_H under reverse faulting stress condition requires the maximum pressure for fracture initiation, which can be found by

$$P_w = 3\sigma_v - \sigma_h \quad (37)$$

It can be seen from Fig. 19 that in a strike-slip stress regime, there is a critical deviation that requires the highest pressure for fracture initiation. When φ is less than the critical deviation, the angular position of fracture $\theta_m = 90^\circ$ and the breakdown pressure is expressed by Eq. (35). When φ is larger than the critical deviation, the angular position of fracture $\theta_m = 0^\circ$ and the breakdown pressure is expressed by Eq. (32).

Considering all the three stress regimes covered in Figs. 2–21, it can be seen that the fracture trace angle never reaches 90°. The condition $\sigma'_\zeta \le \sigma'_\theta$ was never satisfied to initiate transverse fractures. However, special cases have been found in which the most tensile principal stress is independent of θ to facilitate transverse fractures.

5. Concluding remarks

Based on tensile strength criterion ($\sigma'_3 = \sigma_t$), there are two possible conditions under which a transverse fracture can be initiated. (i) The direction of the most tensile principal stress is along the wellbore axis (the fracture trace angle equals ninety degrees). (ii) The most tensile principal stress at breakdown is independent of the circumference of wellbore. It has been shown that the circumferential stress (σ'_θ) will always be smaller than the axial stress (σ'_ζ) in the wellbore wall when hydraulic fractures are initiated. The fracture trace angle never reaches ninety degrees as shown in Table 1. By thorough parametric studies, special cases have been found where the most tensile principal stress at breakdown is independent of the circumference of wellbore. It is observed that transverse fractures can be initiated in those cases.

The results of a thorough investigation of wellbore fracture characteristics have been presented in the form of comprehensive series of dimensionless charts. The charts provide information relating the wellbore fracture initiation pressure, to the angular position and trace angle of fractures in inclined wellbores under in-situ stress conditions corresponding to normal, reverse, and strike-slip faulting. The charts can be used for well completion and fracture system design as well as inverse analysis of in-situ stress from fracturing data. Analytical relations between breakdown pressure and in situ stress are provided whenever possible.

Acknowledgment

The authors wish to acknowledge the support of NSF grant CMMI-0970122 on "GOALI: Probabilistic Geomechanical Analysis in the Exploitation of Unconventional Resources."

References

[1] Hubbert MK, Willis DG. Mechanics of hydraulic fracturing. Trans AIME 1957;210:153–66.
[2] Aadnøy BS. Inversion technique to determine the in-situ stress field from fracturing data. J Pet Sci Eng 1990;4:127–41.
[3] Aadnøy BS. In-situ stress directions from borehole fracture traces. J Pet Sci. Eng 1990;4:143–53.
[4] Haimson BC. The hydraulic fracturing method of stress measurement: theory and practice. In: Hudson JA, editor. Comprehensive rock engineering. Oxford: Pergamon Press; 1993. p. 395–412.
[5] Haimson BE, Cornet FH. ISRM suggested methods for rock stress estimation—Part 3: hydraulic fracturing (HF) and/or hydraulic testing of pre-existing fractures (HTPF). Int J Rock Mech Min Sci 2003;40:1011–20.
[6] Hudson JA, Fairhurst C. Tensile strength, Weibull's theory and a general statistical approach to rock failure. In: Proceedings of the Southampton 1969 civil engineering materials conference; 1969. p. 901–14.
[7] Bredehoeft J, Wolff R, Keys W, Shuter E. Hydraulic fracturing to determine the regional in-situ stress field, Piceance Basin, Colorado. Geol Soc Am Bull 1976;87:250–8.
[8] Haimson BC, Fairhurst C. Initiation and extension of hydraulic fracture in rocks. Soc Pet Eng J 1967;9:310–8.
[9] El-Rabaa W. Experimental study of hydraulic fracture geometry initiated from horizontal wells. In: Proceedings of the SPE 19720. Annual technical conference, San Antonio, TX; 8–11 October 1989. p. 189–204.
[10] Soliman MY. Interpretation of pressure behavior of fractured, deviated, and horizontal wells. In: Proceedings of the SPE 21062. Latin American petroleum engineering conferenec, Rio de Janeiro; 14–19 October 1990.
[11] Weijers L, de Pater CJ, Owens KA, Kogsbøll HH. Geometry of hydraulic fractures induced from horizontal wellbores. SPE Prod. Facilities 1994;9: 87–92.
[12] Fairhurst C. Methods of determining in-situ rock stresses at great depth. TRI-68 Missouri River Division, Corps of Engineer; 1968.
[13] Ljunggren C, Amadei B. Estimation of virgin rock stresses from horizontal hydrofractures. Int J Rock Mech Min Sci Geomech Abstr 1989;26:69–78.
[14] Hoek E, Brown ET. Empirical strength criterion for rock masses. Geotech Eng Div ASCE 1982;106-GT9:1013–35.
[15] Hossain MM, Rahman MK, Rahman SS. Hydraulic fracture initiation and propagation: roles of wellbore trajectory, perforation and stress regimes. J Pet Sci Eng 2000;27:129–49.
[16] Nelson EJ, Meyer JJ, Hillis RR, Mildren SD. Transverse drilling induced tensile fractures in the West Tuna area, Gippsland Basin, Australia: implications for the in situ stress regime. Int J Rock Mech Min Sci 2005;42:361–71.
[17] Kirsch G. Die Theorie der Elastizitaet und die Beduerfnisse der Festigkeitslehre. Z Ver Deutsch Ing 1898;42:797–807.
[18] Bradley WB. Failure of inclined wellbores. J Energy Res Tech Trans AIME 1979;102:232–9.
[19] Daneshy AA. True and apparent direction of hydraulic fractures. Presented at the SPE drilling and rock mechanics conference, paper SPE 3226, Austin, Texas; 5–6 January, 1971.
[20] Aadnøy BS, Bell JS. Classification of drill-induce fractures and their relationship to insitu stress directions. Log Anal 1998;39:27–42.
[21] Barton CA, Moos D, Peska P, Zoback MD. Utilizing wellbore image data to determine the complete stress tensor: application to permeability anisotropy and wellbore stability. Log Anal 1997;38:21–33.
[22] Djurhuus J, Aadnoy BS. In situ stress state from inversion of fracturing data from oil wells and wellbore image logs. J Petrol Sci Eng 2003;38:121–30.
[23] Huang J, Griffiths DV, Wong SW. In situ stress determination from inversion of hydraulic fracturing data. Int J Rock Mech Min Sci 2011;48:476–81.
[24] Aadnoy BS, Belayneh M. Elasto-plastic fracturing model for wellbore stability using non-penetrating fluids. J Pet Sci Eng 2004;45:179–92.
[25] Aadnoy BS, Looyeh R. Petroleum rock mechanics: drilling operations and well design. Gulf Professional Publishing; 2011.
[26] Yew CH, Li Y. Fracturing of a deviated well. SPE Prod Eng 1988;3:429–37.